Anal. Bioanal. Electrochem., Vol. 14, No. 10, 2022, 921-933

Analytical & Bioanalytical Electrochemistry

2022 by CEE
www.abechem.com

Full Paper

Synthesis of MgO Nanoparticle Surfactant Free Modified Carbon Paste Electrode: A Voltammetric Study

K. G. Manjunatha,[1] B. E. Kumara Swamy,[2,*] Gururaj Kudur Jayaprakash,[3] and K. A. Vishnumurthy[1]

[1]*Dept of Industrial Chemistry, Sir M.V. Science College, Bhadravathi, Karnataka (S), India*
[2]*Dept of Studies and Research in Industrial Chemistry, Kuvempu University, Jnana Sahyadri, Shankaraghatta (577451) Shivamoga (D) Karnataka (S), India*
[3]*Department of Chemistry, Nitte Meenakshi Institute of Technology, Bangalore, 560064, Karnataka, India*

*Corresponding Author, Tel.: +91-9900513796
E-Mail: kumaraswamy21@yahoo.com

Received: 17 April 2022 / Received in revised form: 15 October 2022 / Accepted: 15 October 2022 / Published online: 31 October 2022

Abstract- The precipitation method was utilized to prepare MgO nanoparticle (MgO/NPs) without using surfactant in this study, the MgO/NPs was examined by XRD, SEM, and EDS analysis. The MgO/MCPE was developed and used for the oxidation of paracetamol (PA) in presence of ascorbic acid (AA) study by using cyclic voltammetric (CV) and differential pulse voltammetric (DPV) techniques. Finally, the developed sensor shows good electrocatalytic performance in pH and scan rate studies. From the concentration study for the voltammetric determination of PA, the limit of detection was found to be 4.33 µM for PA at MgO/MCPE, the practical purpose of the MgO/MCPE was utilized to evaluate PA in real sample analysis.

Keywords- Ascorbic acid; Paracetamol; MgO nanoparticle; Electrochemical Sensors; Modified carbon paste electrode

1. INTRODUCTION

Paracetamol (PA), Scheme 1, is utilized as an antipyretic and analgesic medication that is used to treat fevers and discomfort [1]. It improves cough and cold symptoms and back,

headache, and toothache discomfort [2]. It's also a non-carcinogenic, and efficient aspirin [3]. PA's toxicity at high doses might lead to hepatotoxicity and nephrotoxicity is related to liver failure. It can also cause skin rashes and inflammation of the pancreas [4]. The widespread therapeutic use of this medicine necessitated the development of quick, easy, and accurate approaches for detecting PA for quality control and medical monitoring [5].

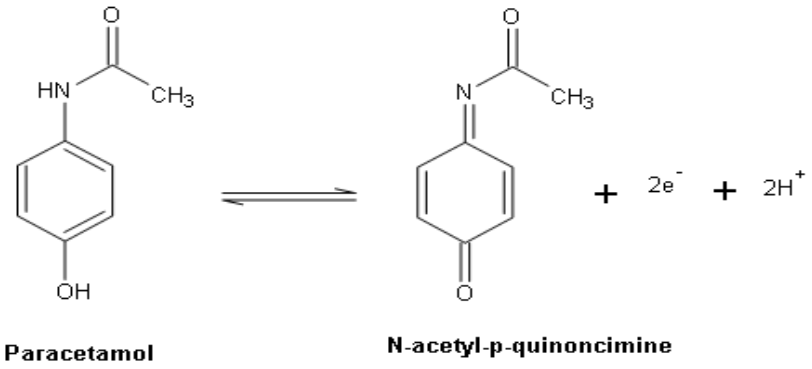

Scheme 1. Oxidation of Paracetamol

Ascorbic acid (AA) is commonly found in various biological systems, foods, drinks, and pharmaceutical goods [6]. The reductive characteristics of ascorbic acid are well known, and it is quickly oxidized to create dehydroascorbic acid [7]. It has the potential to operate as a strong antioxidant in the battle against illnesses caused by free radicals. AA has been used to prevent colds and mental sickness [8]. Excess AA can cause gastrointestinal irritation, while a deficit causes scurvy, which causes a variety of illnesses including Alzheimer's disease, atherosclerosis, cancer, infertility, and HIV infections [9]. The determination of biological substances, for example, high-performance mass spectrometry [10,11], capillary electrophoresis [12], and liquid chromatography [13] have been announced due to their importance.

Because of its significance, analytical technologies such as high-performance mass spectrometry [14], capillary electrophoresis [15], and liquid chromatography [16] have been proclaimed for the determination of biological substances [17]. However, these activities are difficult because of the difficult sample preparation, high cost, and need for quick analysis. In contrast to these sophisticated approaches, Electrochemical sensors have gotten a lot of attention because of their rapid and quick reaction, clarity in the experimental procedure, strong stability, low detection limit, outstanding repeatability, and inexpensive cost [18]. Carbon paste electrodes have been used as electrodes in recent years due to their simple creation, rapid reaction, and good sensitivity [19,20].

Magnesium nanoparticles are employed in a variety of applications, including electronics, catalysis, ceramics, petrochemical products, hazardous waste remediation, paints,

superconducting goods, optical, antimicrobial, and antibacterial activity [21,22]. MgO/NPs are an excellent wide-bandgap insulator with applications in catalysis, hazardous waste remediation, refractory, paint, transparent ceramics, absorbent for numerous pollutants, and superconductor goods [23,24]. Furthermore, MgO/NPs appear to be excellent building blocks for the creation of functional nanostructures or as a model compound for the study of surface reactivity on oxides.

Due to the quantum confinement effect, its nanostructures are projected to exhibit unique characteristics that are superior to their bulk counterparts [25-27]. As a result, several in-depth investigations have been conducted to synthesize nanoscale. MgO/NPs have been synthesized utilizing a variety of techniques, including sol-gel, combustion, co-precipitation, and spray pyrolysis [29-30].

In the previous study [31], the synthesis of MgO nanoparticles with surfactant and in this work, without adding surfactant in the preparation of MgO/NPs was examined to determine PA in the presence of AA utilizing CV and DPV methods.

2. EXPERIMENTAL SECTION

2.1. Reagents

The chemicals AA and PA were got from Himedia. The stock solution was prepared from double distilled (DD) water. The phosphate buffer solution (PBS) was prepared by mixing the stoichiometric ratio of $NaH_2PO_4 \cdot H_2O$ and Na_2HPO_4. All aqueous solutions were prepared with DD water.

2.2. Equipment

Electrochemical experiments were carried out with a CHI-660c (CH Instrument-660 electrochemical workstation). Bare and MgO/MCPE were used for working electrodes. The platinum electrode act as a counter electrode and the saturated calomel electrode (SCE) as a reference electrode.

2.3. Synthesis of MgO nanoparticle

The synthesized MgO nanoparticles results were already reported in the previous paper with reference number [31].

2.4. Fabrication of BCPE and MgO/MCPE

The bare carbon paste electrode (BCPE) was prepared by hand mixing 70% graphite powder and 30% silicone oil in an agate mortar for about 30 minutes to get a homogeneous carbon paste obtained. In addition, the Magnesium Oxide modified carbon paste electrode

(MgO/MCPE) was made by mixing 61% graphite powder, 2 mg of 6% MgO/NPs, and 33% silicone oil in an agate mortar to make a homogenous carbon paste. The paste was then packed into the end of a 3 mm internal diameter polyvinyl tubing (PVC) tube and smoothed out on tissue paper to create a new surface. Similarly, the 4, 6, and 8 mg of MgO/MCPE were synthesized in the same manner described above.

3. RESULTS AND DISCUSSION

3.1. Characterization of MgO nanoparticle

The MgO nanoparticle characterized data results were already discussed in the previous paper with reference number [31].

3.2. Comparative study for BCPE and different amounts (MgO/MCPE)

Figure 1 depicts the electrochemical behavior of PA at MCPE in the presence of PBS solution investigated and compared with BCPE, the oxidation curve of PA at BCPE showed a reversible nature. The CVs with MCPE, in the presence of 2 mg of MgO/NPs showed well-defined redox peaks obtained with the MgO/MCPE, and the addition of 4 mg of MgO/MCPE showed significant empowerment in the peak current. Further, 4 mg MgO/MCPE demonstrates increasing peak current comparatively more than other modified electrodes. Finally, the 6 mg of MgO/MCPE decreased the redox peak current. Therefore, 4 mg of MgO/MCPE shows more sensitivity and choose for further parameter studies.

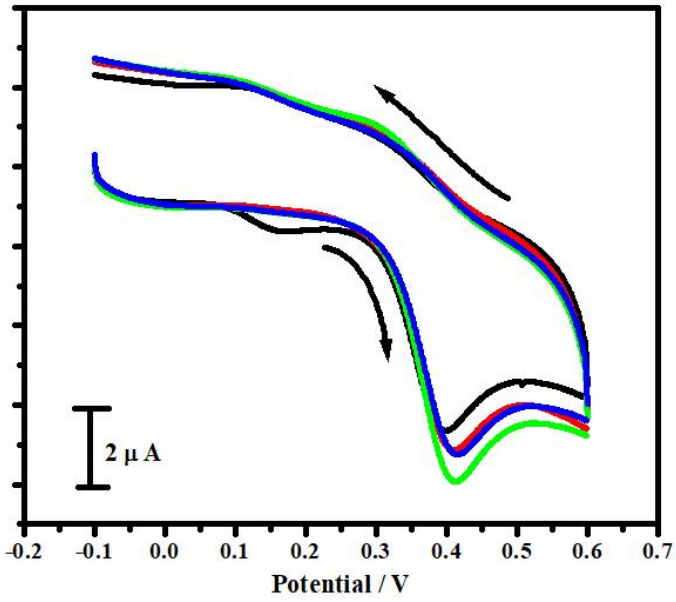

Figure 1. Cyclic voltammograms obtained for BCPE and different amounts of MgO/MCPE

3.3. Electrocatalytic nature of PA at BCPE and MgO/MCPE

In the analysis of PA, both BCPE and MgO/MCPE are used. The voltammograms for 10 µM PA in 0.2 M PBS at a scan rate of 50 mVs^{-1} at MgO/MCPE, the dotted line (BCPE), and the solid line (MCPE), The BCPE show poor electrochemical response with showed peak potential at 0.38 V. The MgO/MCPE indicating a significant enhancement of anodic peak current and observed peak potential at 0.32 V are shown in Figure 2. Thus, from the above results the MgO/MCPE proved more sensitivity and more electrocatalytic activity toward the determination of PA.

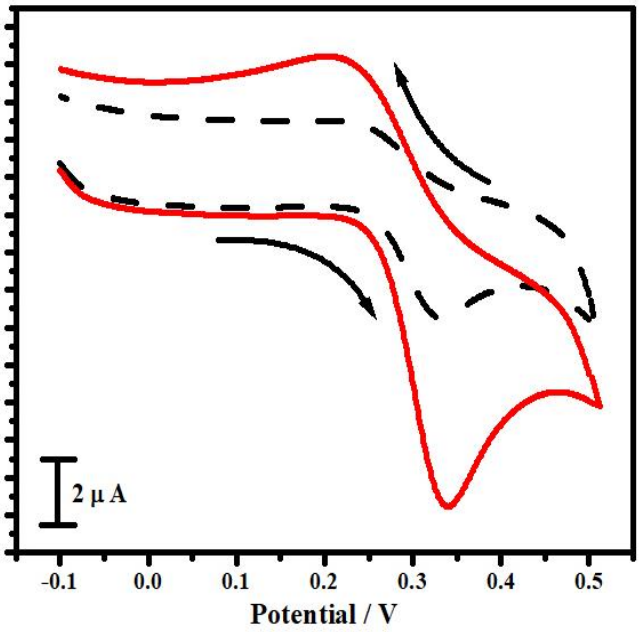

Figure 2. CVs obtained for 10µM PA at BCPE (dotted line) and MgO/MCPE (solid line) in 0.2 M PBS at scan rate 50mVs^{-1}

3.4. Impact of pH variation at MgO/MCPE

The MgO/MCPE is used to investigate the effect of pH on PA oxidation. The acquired CVs for PA in the pH range of 5.8–7.8 are shown in Figure 3A. The graph defined that as the pH changed from 5.8, 6.2, 6.6, 7.0, 7.4, and 7.8. The peak potential drifted to the negative side. In Figure 3B the slope value of 75 mV/pH is near the Nernstian value of 59 mV. This result indicates that an equal number of electrons and proton transfers occurred.

3.5. Impact of sweep rate at MgO/MCPE

To see how sweep rates influenced PA oxidation, the MgO/MCPE was used. The 10 µM PA was tested at scan speeds from 0.05 to 0.5 Vs^{-1}. Figure 4A showed as the sweep rate increases with increasing the anodic peak current and the anodic peak potential moved towards

the more positive side. Figure 4B displays the graph of I_{pa} versus sweep rate, and the results show good linearity, with the observed correlation coefficient R^2=0.9964 and the Figure 4C square root of sweep rate R^2=0.9891, from this study implying that the adsorption electrode process.

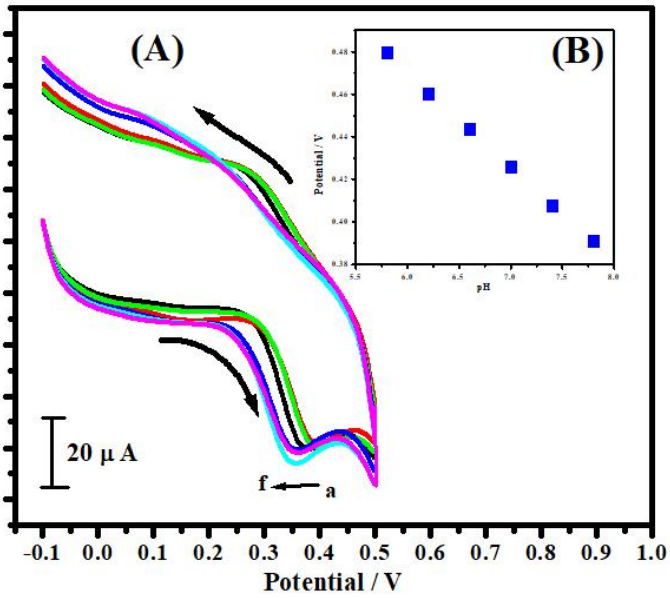

Figure 3. (A) CVs obtained for 10µM PA with different pH from 5.8 to 7.8 at scan rate 50 mVs^{-1}; (B) Plot of Epa v/s different pH

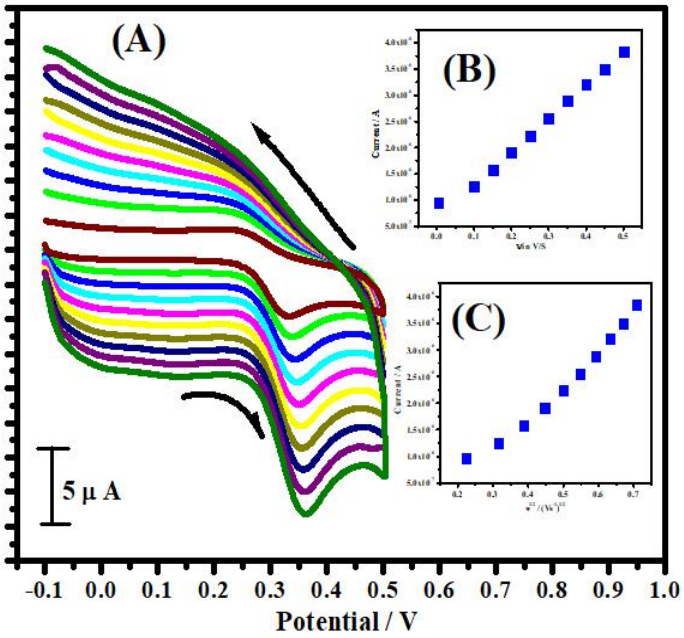

Figure 4. (A) CVs of 10µM PA in pH 7.4 at MgO/MCPE, at varied sweep rates from 0.05, to 0.5 V s^{-1}; (B) Plot of I_{pa} of PA v/s different sweep rate; (C) Plot of I_{pa} of PA v/s square root of scan rate

3.6. Impact of concentration at MgO/MCPE

The voltammograms taken for various concentrations of PA from 10 to 100 µM are shown in Figure 5A. The voltammograms in Figure 5B show a rise in anodic peak current increases with increasing in PA concentrations from 10 to 100 µM, indicating that the concentration influences PA oxidation.

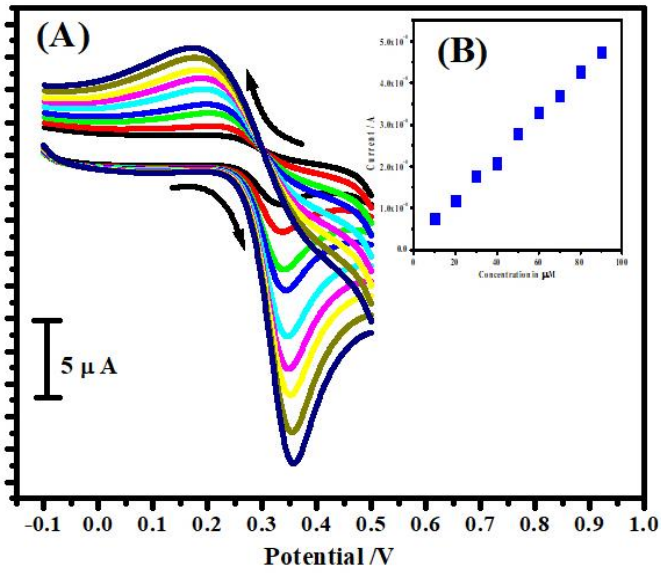

Figure 5. (A) CVs on MgO/MCPE in PBS (pH 7.4) with varied PA concentrations from 10 to 90 µM; (B) Linear graph of Ipa v/s varied concentration of PA

The correlation coefficient R^2= 0.9994 was discovered, and the LOD [32] is 4.33 µM and the LOQ [32] is 14.36 µM was used to compute the detection limit. Where 'M' is the slope and 'S' is the standard deviation from the calibration plots. The detection limit of PA at MgO/MCPE and other reported modified electrodes were shown in Table 1.

Table 1. The comparison of LOD for PA with the other reported electrodes

Sl. No	Electrode	Detection limit (µM)	Technique	References
1	Pd/ Al	5.0	DPV	[34]
2	MgO/TX-100/MCPE	6.2	CV	[35]
3	Bi_2O_3/GCE	5.05	CV	[36]
4	TiO_2/MCPE	5.2	CV	[37]
5	MgO/MCPE	4.3	CV	This work

3.7. Electrochemical characterization of AA at BCPE and MgO/MCPE

Figure 6 displays the CVs of 10 µM AA at BCPE and MgO/MCPE. At the BCPE of AA (dashed line) showing a poor peak, current response and oxidation take place at 0.231 V. On the other hand, MgO/MCPE (solid line) increases the peak current response more, and the peak potential at 0.184 V compared to that of BCPE. This result suggests the MgO/MCPE improved more electrocatalytic activity than BCPE.

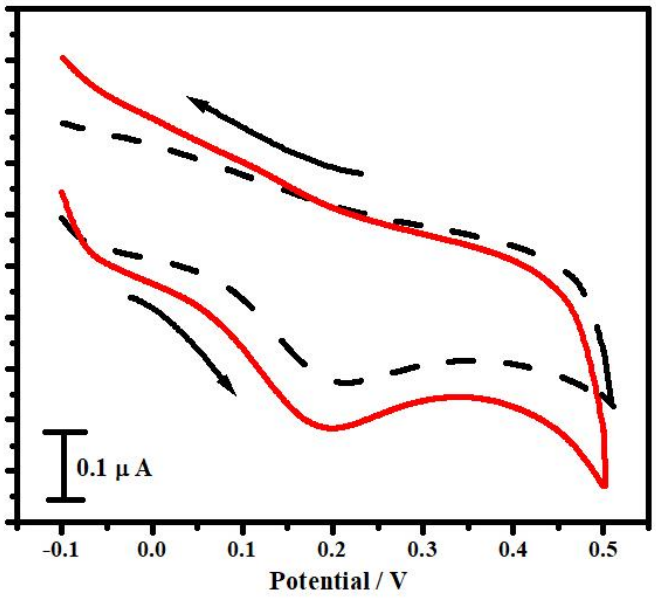

Figure 6. CVs, of 10 µM AA in pH 7.4 at BCPE and MgO/MCPE are represented as a dotted line and a solid line respectively

3.8. Impact of scan rate of AA at MgO/MCPE

The influence of scan rate on the electrochemical property of AA was studied at MgO/MCPE. As shown in Figure 7A, a series of voltammograms were created at various scan speeds ranging from 0.05 to 0.5 Vs^{-1}. Figure 7B indicates that as the scan rate rises, so does the peak current (I_{pa}) of AA, demonstrating a linear relationship. Figure 7C shows that the electrode process of AA at the MgO/MCPE is an adsorption-controlled process (R^2=0.9909) and the linear regression value (R^2=0.9987).

3.9. Impact of concentration of AA at MgO/MCPE

At MgO/MCPE, the effect of concentration on AA oxidation was investigated. As the concentration grows, the anodic peak current rises with it, as seen in Figure 8A. The curve of I_{pa} against concentration is shown in Figure 8B. R^2=0.9904 was determined to be the correlation coefficient. The LOD and LOQ are 11.7 and 35.5 M, respectively [33].

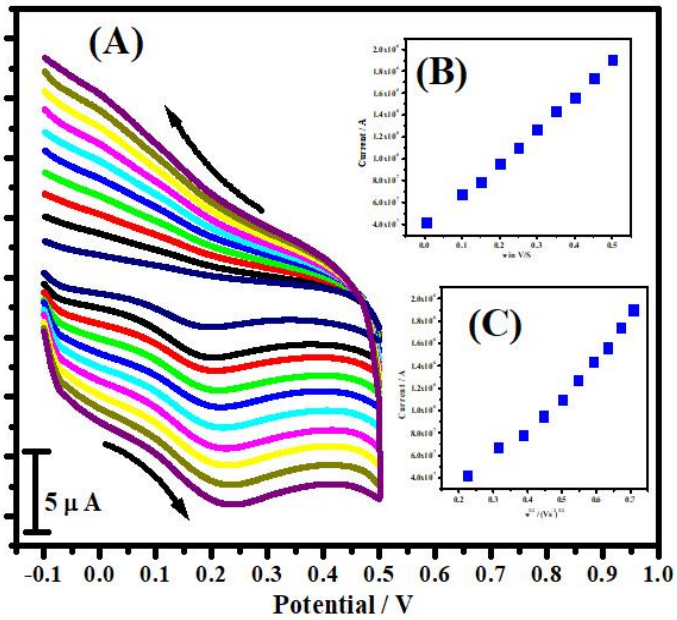

Figure 7. (A) CVs of 10 µM AA at varied scan rates from 0.05– 0.5 V s^{-1}; (B) plot of I_{pa} of AA versus different scan rates; (C) plot of I_{pa} of AA versus square root of scan rates

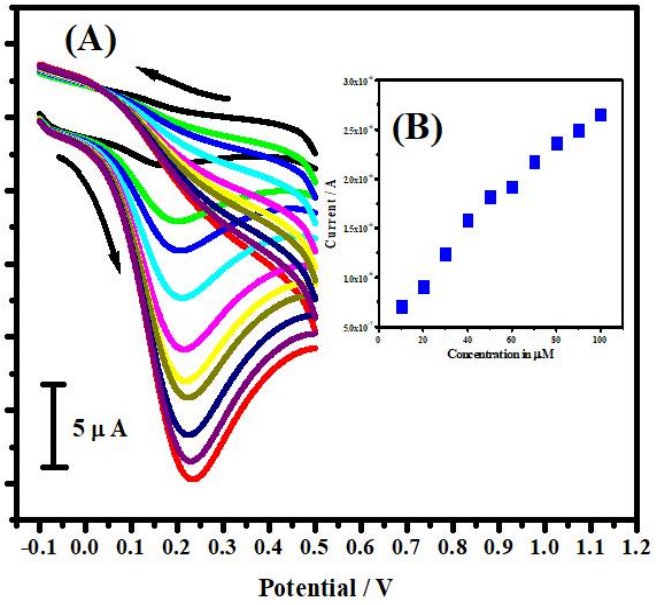

Figure 8. (A) CVs of MgO/MCPE in 0.2M PBS solution at different concentrations of (10 µM to 90 µM) of AA with scan rate 50 mV s; (B) Plot of I_{pa} of AA v/s different concentrations of AA

3.10. Simultaneous determination of AA and PA

The MgO/MCPE and BCPE were utilized to examine AA in the presence of PA. Figure 9 depicts the dotted line indicating BCPE, and the solid line represents MgO/MCPE. In the

simultaneous determination of AA and PA, the current response of BCPE is poor, but the current response of MgO/MCPE is better, with two well-defined oxidation peak potentials of 0.15 V for AD and 0.28 V for PA, implying that the electrochemical nature of MgO/MCPE is superior to BCPE in sensing AA and PA.

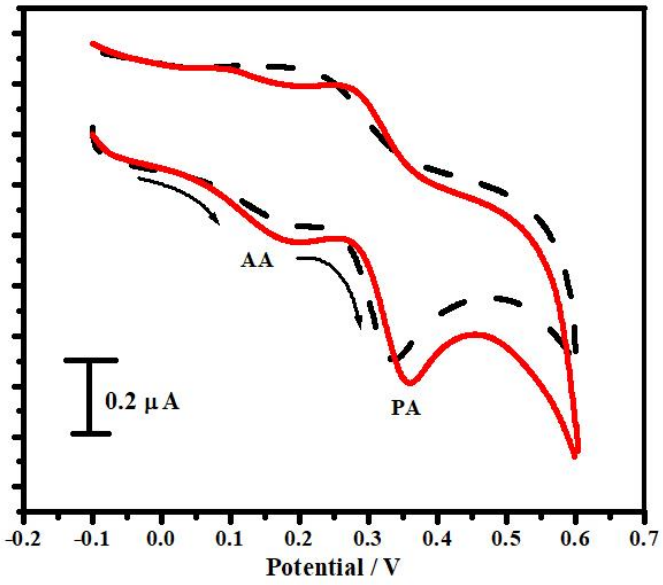

Figure 9. CVs of a binary mixture of PA and AA in 0.2M PBS of pH 7.4 at BCPE (dotted line) and MgO/MCPE (solid line) at scan rate 50 mV s^{-1}

3.11. Interference analysis of AA and PA

Paracetamol is thought to be a possible ascorbic acid interfering substance. The interference research at MgO/MCPE was carried out using the differential pulse voltammetric (DPV) method. CVs for two compounds (PA and AA) in PBS in pH 7.4 at a sweep rate of 50 mVs^{-1} are shown in Figure 10A and Figure 10B. The anodic peak current of PA is steadily increasing owing to an increase in PA concentration alone, whilst the peak current of AA stays constant in Figure 10a. Similarly, in Figure 10b anodic peak current of AA increases with increasing concentration of AA while keeping the PA constant. The measured voltammograms led to the conclusion that PA and AA oxidation occurs independently of one another, resolving the issue of interference in MgO/MCPE.

3.12. Real sample analysis

The PA tablet (Dolo-650) sample was bought from Harson Laboratories, and the tablet sample was diluted in PBS (0.2 M) to achieve the desired concentration. The percentage recoveries obtained from the experimental findings reveal good recovery at the MgO/MCPE, which is given in Table 2.

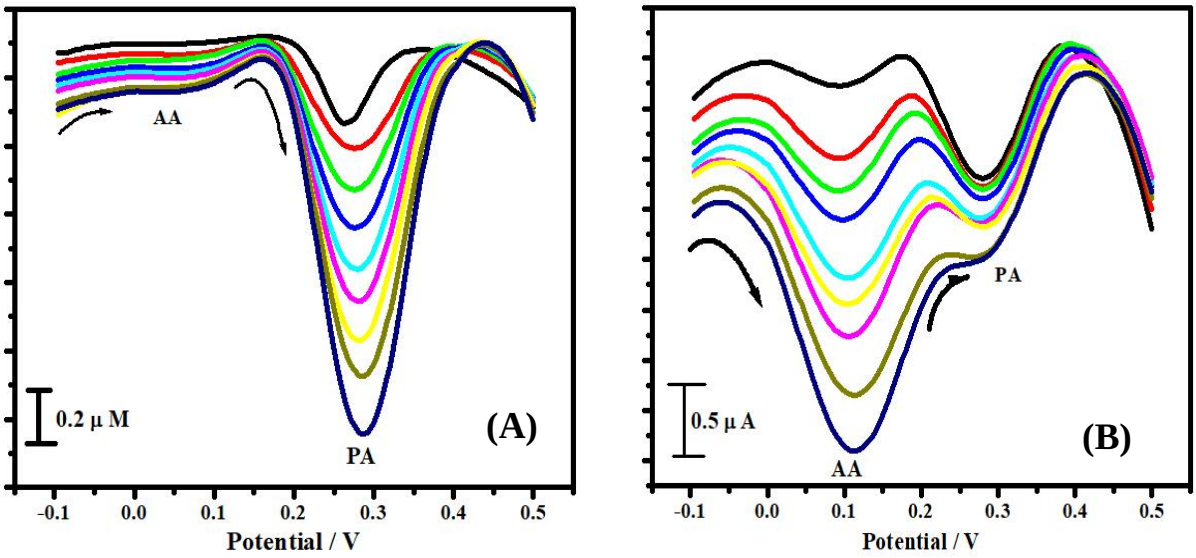

Figure 10. (A) DPVs of PA in 0.2 M PBS of pH 7.4 at MgO/MCPE with different concentrations in the range of 10 to 90 µM; (B) DPVs of PA in 0.2 M PBS of pH 7.4 at MgO/MCPE with different concentrations in the range of 10 to 90 µM

Table 2. Detection of PA in tablet sample at MgO/MCPE (n=3)

Sample	PA added (µM)	Found (µM)	Recovery (%)
PA tablet	10	9.85	97.23
	20	18.62	94.42
	30	28.13	96.51

4. CONCLUSION

The MgO nanoparticle was produced using the precipitation process without using surfactant in this study, and then spectroscopically characterized. The MgO/MCPE has shown good electrocatalytic effects on PA and AA oxidation as evidenced by the scan rate which reveals that both have a heterogeneous rate constant. The concentration study determines the detection limit for PA was 4.33 µM and 11.7 µM limit of quantification, respectively. The interference investigation revealed that PA and AA oxidation were independent of one another. As a result, the MgO/MCPE appears to be a viable method for determining additional neurotransmitters.

REFERENCES

[1] R. Sandulescu, S. Mirel, and R. Oprean, J. Pharm. Biomed. Anal. 23 (2000) 77.

[2] X. D. Shang Guan, H. F. Zhang, and J. B. Zheng, Anal. Bioanal. Chem. 391 (2008) 1049.
[3] I. Noviandri, and R. Rakhmana, Int. J. Electrochem. Sci. 7 (2012) 4479.
[4] C. Y. Li, G. Q. Zhan, Q. D. Yang, and J. J. Lu, Bull. Korean Chem. Soc. 27 (2006) 1854.
[5] C. S. Erdurak-Kilic, B. Uslu, B. Dogan, U. Ozgen, S. A. Ozkan, and M. Coskun, J. Anal. Chem. 61 (2006) 1113.
[6] H. Sies, W. Stahl, and A. R. Sundqiust, Ann. N. Y. Acad. Sci. 669 (1992) 7.
[7] S. J. Padayatty, A. Katz, Y. Wang, P. Eck, O. Kwon, J-H. Lee, and S. Chen, J. Am. Coll. Nutr. 22 (2003) 18.
[8] B. A. Fox, A. G. Cameron, Food Science, Nutrition and Health, 5th edition, Edward Arnold, London, UK, 1989.
[9] J. Du, J. J. Cullen, and G. R. Buettner, Biochim. Biophys. Acta 1826 (2012) 443.
[10] I. Stone, and J. Orthomol. Psychiatry 1 (1972) 82.
[11] V. Valpuesta, and M. A. Botella, Trends Plant. Sci. 9 (2004) 573.
[12] K. R. Mahanthesha, and B. E. Kumara Swamy, J. Electroanal. Chem. 703 (2013) 1.
[13] M. Kumar, B. E. Kumara Swamy, Sathish Reddy, Wei Zhao, S. Chethana, and V. Gowrav Kumar, J. Electroanal. Chem. 835 (2019) 96.
[14] T. S. Sunil Kumar Naik, Muthui Martin Mwaurah, and B. E. Kumara Swamy, J. Electroanal. Chem. 843 (2019) 71.
[15] K. V. Harisha, B. E. Kumara Swamy, P.S. Ganesh, and H. Jayadevappa. J. Electroanal. Chem. 832 (2019) 486.
[16] A. Anil Kumar, B. E. Kumara Swamy, T. Shobha Rani, P. S. Ganesh, and Y. Paul. Raj. Mater. Sci. Eng. C 98 (2019) 746.
[17] Q. Wan, X. Wang, F. Yu, X. Wang, and N. Yang, J. Appl. Electrochem. 39 (2009) 785.
[18] G. K. Jayaprakash, and R. Flores-Moreno, Electrochim. Acta. 248 (2017) 225.
[19] J. G. Manjunatha, B. E. Kumara Swamy, M. Deraman, and G. P. Mamatha, Der. Pharma Chemica 4 (2012) 2489.
[20] G. Tigari, and J. G. Manjunatha, J. Anal. Testing 3 (2019) 331.
[21] A. H. Wani, and M. A Shaah. J. Applied Pharm. Sci. 2 (2012) 40.
[22] Verlag Berlin Heidelberg. Mathibela Elias Aphane. S. Krishna Moorthy et al. Materials Today: Proceedings 2 (2015) 4360.
[23] C. Henrist, J. P. Mathieu, C. Vogels, A. Rulmont, and R. Cloots, J. Crystal Growth 249 (2003) 321.
[24] X. Tran, X. Phuoc, T. Phuoc, H. Howard, V. Donald Martello, Y. Soong, and K. M. Chyu, Optics and Lasers in Engin. 46 (2008) 829.
[25] I. Cakmak, and H. Marschner. Plant Physiology 98 (1992) 1222.
[26] D. Kumar, V. Buchi Reddy, G. B. Mishra, R. K. Rana, N. M. N. Rajender, and S. Varma, Tetrahedron 63 (2007) 3093.

[27] M. Khodakovskaya, E. Dervishi, M. Mahmood, Y. Xu, Z. Li, F. Watanabe, and A. S. Biris, ACS Nano 3 (2009) 3221.
[28] S. Lin, J. Reppert, Q. Hu, J. S. Hudson, M. L. Reid, T. A. Ratnikova, A. M. Rao, H. Luo, and P. C. Ke. Uptake, Inter. Sci. Small 10 (2009) 1128.
[29] L. Zheng, F. Hong, and S. C. Liu, Biol. Trace Element Res. 104 (2005) 83.
[30] K. R. Mahanthesha, and B. E. Kumara Swamy, J. Electroanal. Chem. 703 (2013) 1.
[31] K. G. Manjunatha, B. E. KumaraSwamy, H. D. Madhuchandra, K. J. Gururaj, and K. A. Vishnumurthy, Sens. Inte. 2 (2021) 100127.
[32] H. D. Madhuchandra, and B. E. Kumara Swamy, Chem. Data Collect. 28 (2020) 100447.
[33] P. S. Ganesh, B. E. Kumara. Swamy, and A. B. Teradale, Anal. Bioanal. Electrochem. 5 (2018) 612.
[34] M. H. Pournaghi-Azar, and A. Saadatirad, Electroanalysis 22 (2010) 1592.
[35] K. G. Manjunatha, B. E. KumaraSwamy, H. D. Madhuchandra, K. J. Gururaj, and K. A. Vishnumurthy, Sens. Inte. 2 (2021) 100127.
[36] A. A. Pasban, E. H. Nia, and M. Piryaei, J. Nanoanal. 4 (2017) 142.
[37] K. G. Manjunatha, B. E. Kumara Swamy, H. D. Madhuchandra, and K. A. Vishnumurthy, Chem. Data Collect. 31 (2021) 100604.